Biochimie 92 (2010) 772–778

Contents lists available at ScienceDirect

Biochimie

journal homepage: www.elsevier.com/locate/biochi

Research paper

Analysis of bacterial RNase P RNA and protein interaction by a magnetic biosensor technique

Dan Li, Martin H.F. Meyer, Dagmar K. Willkomm, Michael Keusgen, Roland K. Hartmann*

Institut für Pharmazeutische Chemie, Philipps-Universität Marburg, Marbacher Weg 6, D-35037 Marburg, Germany

ARTICLE INFO

Article history:
Received 4 November 2009
Accepted 16 February 2010
Available online 6 March 2010

Keywords:
Bacterial RNase P
RNA–protein interaction
Magnetic detection
Magnetic beads

ABSTRACT

A magnetic sensor technique was applied to analyze the interaction of immobilized bacterial RNase P protein and 3′-biotinylated RNase P RNA bound to streptavidin-coated magnetic beads. Our measurements with three types of beads from different suppliers resulted in K_d values of about 1–2 nM (at 4.5 mM Mg^{2+} and 150 mM NH_4^+) for *Escherichia coli* RNase P RNA and protein, consistent with previous analyses using different techniques. We further measured affinity of the *E. coli* RNase P protein to chimeric RNase P RNA variants, consisting of an *E. coli* specificity domain and an engineered archaeal catalytic domain. A "bacterial-like" 1-bp insertion and 2-nt deletion in the helix P2/P3 region largely improved affinity, providing independent evidence that these elements are crucial for interaction of the two RNase P subunits. Moreover, our study documents that the properties of the streptavidin-coated magnetic beads decide on success or failure of the technique.

1. Introduction

Ribonuclease P (RNase P) catalyzes the endonucleolytic 5′ end maturation of tRNA primary transcripts [1–4]. Bacterial RNase P enzymes are composed of a catalytic RNA subunit, ~400 nucleotides (nt) in length, and a single small protein of typically 120 amino acids that contributes about 10% to the molar mass of the ribonucleoprotein enzyme [5,6]. The protein is essential *in vivo* (reviewed in [7]), but *in vitro* its absence can be compensated for by increased mono- and particularly divalent cations [5]. In contrast to bacteria, archaeal RNase P enzymes consist of an RNA subunit with no or very residual RNA-alone activity *in vitro* [8]; the RNA subunit requires complexation with at least four protein cofactors for optimal activity [9].

Three studies have so far reported quantitative binding data for complex formation between bacterial RNase P RNA (P RNA) and its protein cofactor (P protein): Vioque et al. [10] determined a K_d of 0.4 nM for *Escherichia coli* P RNA–protein interaction at 10 mM $MgCl_2$ and 400 mM NH_4Cl. This was accomplished by a nitrocellulose filter binding assay, exploiting the fact that P protein, but not the RNA–protein complex, adsorbs to the membrane. An identical K_d value for *E. coli* P RNA and protein was obtained with a gel retardation assay [11] under very similar ionic conditions. The third study [12] analyzed the interaction between P RNA and P protein of *Bacillus subtilis* by a magnetic capture assay, using radiolabeled P RNA and His-tagged P protein immobilized to magnetic agarose beads containing nickel coordinated by nitrilotriacetic acid (NTA, Qiagen). At intermediate ionic strength (50 mM Tris–HCl, pH 8, 10 mM imidazole, 10 mM $MgCl_2$, and 100 mM KCl), a K_d of 15 nM was measured, with either C- or N-terminally His-tagged protein.

Our goal was to measure K_d values for P RNA variants with a broad spectrum of P protein affinities [13], including chimeric bacterial/archaeal P RNAs with less functional archaeal catalytic domains. We refrained from applying the nitrocellulose binding assay since it requires the use of ^{35}S-labeled P protein [10]. We were also skeptical about the gel retardation assay [11] because (i) such assays have rather narrow affinity windows in which gel-resolvable complexes stably form and can be used to determine K_d values [14], (ii) they do not measure real equilibrium dissociation constants due to the "caging" effect, and (iii) assay conditions during preincubation to form the complex are usually non-identical to those during electrophoresis [11,12]. We thus tried to adapt the magnetic capture assay [12] for our purposes, but did not succeed, possibly due to the use of non-identical batches of magnetic beads.

This prompted us to adopt an in-house-developed magnetic sensor approach ([15] and Fig. 1D, see detailed description in the figure legend) that had been successfully applied to the sensitive quantitation of the C-reactive protein (CRP) in human body fluids, which serves as a marker for inflammatory processes [16]. For our purposes, 3′-biotinylated P RNAs were immobilized on commercially available, streptavidin-coated magnetic beads [16,17] (Fig. 1). The P protein was bound by adsorption to a solid phase filter (sintered polyethylene) contained in a special polycarbonate capsule (merchandised as ABICAP® columns, SENOVA). Magnetic beads that bound to the column via P RNA – P protein interaction were detected by the so-called frequency mixing detection technique (Fig. 1) [15].

* Corresponding author. Tel.: +49 6421 2825827; fax: +49 6421 2825854.
E-mail address: roland.hartmann@staff.uni-marburg.de (R.K. Hartmann).

0300-9084/$ – see front matter © 2010 Elsevier Masson SAS. All rights reserved.
doi:10.1016/j.biochi.2010.02.018

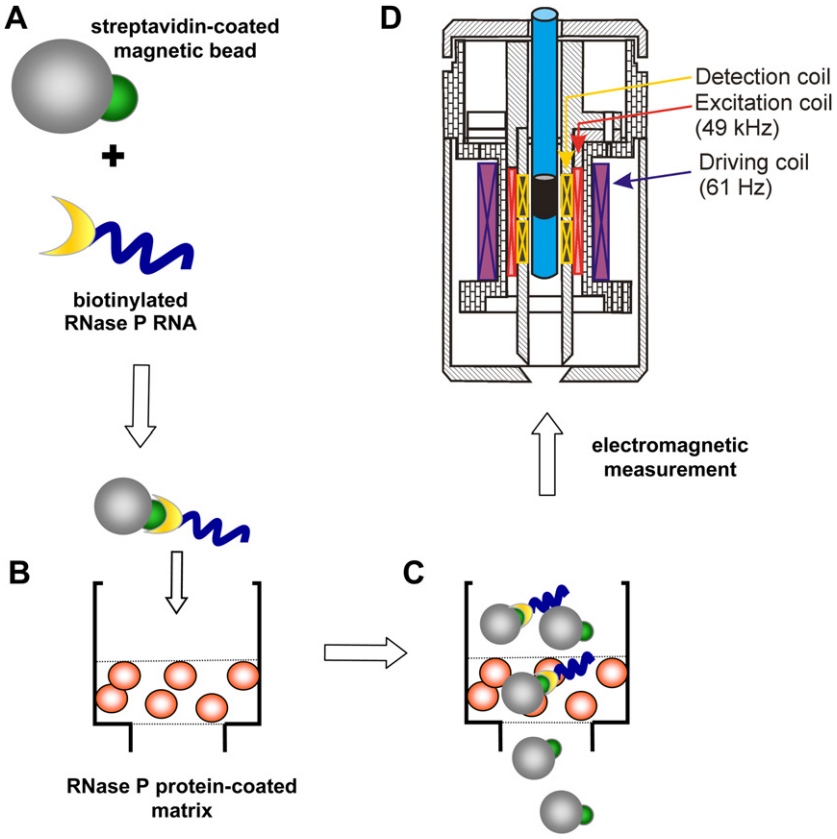

Fig. 1. Illustration of the experimental setup. (A) 3′-biotinylated P RNAs (blue lines with yellow sickle) were bound to streptavidin-coated magnetic beads (grey spheres with green cap). (B) *E. coli* P protein (orange spheres) was adsorbed to the polyethylene matrix and the P RNA/bead solution was loaded onto the column. (C) P RNA–bead complexes are retained on the column via P RNA–P protein interaction. (D) Section of the sensor head: the polycarbonate column (cyan) containing the ABICAP® filter (black); the two excitation coils are shown in blue and red, and the two detection coils are depicted in yellow on black background. Applying a two-frequency magnetic field excitation, the magnetic response was detected at a third frequency which is a linear combination of the applied frequencies [15]. The mixing signals were generated exclusively by the magnetic beads because they are the only components in the system with a non-linear magnetization curve [15]. The magnetic beads were exposed to the magnetic field generated by two excitement coils with frequencies of 61 Hz and 49 kHz, respectively, in one measurement head. One detection coil is positioned at the level of the sintered polyethylene filter (the measuring coil) and the second below (the reference coil) to measure the background (blank) value that is subtracted from the first. The two detection coils are balanced, such that the directly induced signal vanished in the absence of beads. The output voltage signal was shown to be linear for four orders of magnitude in iron concentration (between 0.1 and 1000 mg iron per liter) [15]. The measurement head used for the advanced and high sensitivity detection of magnetic beads was developed by the Research Center Jülich, Germany, and SENOVA GmbH, Jena, Germany. (For interpretation of the references to colour in this figure legend, the reader is referred to the web version of this article.)

The results presented here indicate that the magnetic sensor technique is suitable for the measurement of specific RNA–protein interactions. Affinities determined with this technique for complexes formed between the *E. coli* P protein and different chimeric P RNA variants containing an engineered archaeal catalytic domain nicely corresponded to similar analyses utilizing other approaches. Streptavidin-coated magnetic beads from some suppliers could in principle be used for the technique, whereas others failed to give reasonable results. We also found that the use of specific batches of magnetic beads from the same supplier decided on the success or failure of our measurements.

2. Material and methods

2.1. Chemicals

Water was obtained from a Millipore® unit. All other chemicals were purchased from standard commercial sources at analytical grade.

2.2. Magnetic beads

The magnetic biosensor technique applied here requires the use of superparamagnetic beads, i.e. beads with entirely reversible magnetization. Beads were received from the following suppliers:

1. Chemagen GmbH (Baesweiler, Germany) type M-PVA SAV1 NCO; diameter 0.5–1.0 μm; streptavidin coating via isocyanate [NCO] coupling to the surface of superparamagnetic polyvinyl alcohol beads; binding capacity: ≥400 pmol biotinylated oligonucleotide/mg beads; magnetite: 50–60%.
2. Invitrogen (Karlsruhe, Germany) type Dynabeads® M-270 Streptavidin beads; diameter 2.8 μm; streptavidin monolayer covalently coupled to a hydrophilic surface based on carboxylic acid beads; binding capacity: ∼200 pmol single-stranded oligonucleotide or ∼10 μg double-stranded DNA per mg of streptavidin-coated beads; for oligonucleotides, capacity is inversely related to molecule size; iron content (ferrites): 14% (20%).
3. Merck Estapor® Fontenay-sous-Bois, France) type BE-M0.8/26: diameter 2.6 μm, ferrite 30%; streptavidin covalently coupled to a high density carboxylic acid surface; binding capacity: ≥400 pmol of biotinylated oligonucleotides per mg of beads.
4. Thermo Scientific Seradyn (Indianapolis, USA) type MG-SA: diameter of 1.0 μm, carboxylate-modified particles covalently coated with streptavidin; binding capacity: 1–5 nmol biotin/mg of beads; 40% magnetite.

All magnetic beads were pre-coated with streptavidin by the manufacturer.

2.3. Columns

All measurements were performed using small plastic columns (volume 0.75 ml) which contained ABICAP® polyethylene (PE) sintered filters. These had a pore diameter of 50 μm. ABICAP® sintered filters and columns were received from SENOVA GmbH (Jena, Germany).

2.4. RNase P protein and RNA

E. coli P protein and P RNA were prepared precisely as described in [13]. Briefly, the protein was overexpressed in *E. coli* with an N-terminal hexahistidyl tag and purified by Ni-NTA affinity chromatography; the RNA subunit was produced by run-off *in vitro* T7 transcription from plasmid pDW98 linearized with BsaAI. 3′ terminal biotinylation of P RNA was performed by periodate oxidation of the RNA's 3′ terminal ribose *cis*-diol and subsequent reaction with biotinamidocaproyl hydrazide as described [18]: In detail, 3–4 nmol RNA were incubated in 100 μl of 40 mM KIO_4 for 1 h at room temperature in the dark. The reaction was stopped by addition of an equal volume of 50% ethylene glycol and ethanol precipitation. The dried pellet was dissolved in 100 μl of 10 mM biotinamidocaproyl hydrazide and incubated for 2 h at 37 °C, followed by addition of 100 μl of 0.2 M $NaBH_4$ and 200 μl of 1 M Tris–HCl pH 8.2, and incubation for 30 min at 37 °C in the dark. The RNA was finally purified by gel chromatography using Sephadex™ G-75 and Microspin™ columns (Amersham Pharmacia). Binding of P protein and P RNA was assayed in a buffer previously used for RNase P holoenzyme processing assays (KN4.5 buffer, containing 20 mM HEPES–KOH pH 7.4, 4.5 mM $Mg[OAc]_2$, 150 mM NH_4OAc, 2 mM spermidine, 0.05 mM spermine and 4 mM β-mercaptoethanol; [13]).

2.5. P protein immobilization

E. coli P protein was immobilized on the sintered polyethylene filters by adsorption based on hydrophobic interaction, comparable with protein adsorption to microtiter plates. ABICAP® columns were first washed with degassed ethanol (96%), then several times with ethanol–water (50/50), followed by several washing steps with immobilization buffer (carbonate buffer, pH 9.5, 0.1 M). P protein was immobilized for 1 h using 0.5 ml immobilization buffer per column that contained 5 mg (0.385 nmol) P protein. The amount of protein adsorbing to the matrix could not be determined with sufficient sensitivity by quantitation according to Bradford [19]. However, the protein loading capacity of the used ABICAP® filters was previously determined to be about 270 pmol using a fluorescent model protein (DsRed) [20]; assuming that the P protein bound with similar efficiency, P protein was in excess over P RNA in the tested concentration range. Finally, ABICAP® columns were blocked using casein 5.5 mg/ml in PBS-buffer (0.12 M NaCl, 30 mM phosphate [Na_2HPO_4/NaH_2PO_4] pH 7.3) and were then ready-to-use. All steps were performed under conditions of gravity flow.

2.6. Measurements

Ready-to-use ABICAP® columns were washed using 0.5 ml of KN4.5 buffer (see above). Defined amounts of P RNA were diluted in KN4.5 buffer, followed by incubation for 5 min at 55 °C and 25 min at 37 °C. The P RNA solution was then gently mixed with a constant amount of diluted (1:100 v/v) magnetic beads suspension in KN4.5 buffer and incubated for additional 30 min at room temperature. Then 0.5 ml of the P RNA/magnetic beads suspension was allowed to enter the sintered polyethylene filter (ABICAP®) by gravity flow; when the brownish bead solution had reached the bottom of the filter, the flow was stopped followed by incubation for 30 min at room temperature. Then the filter was washed using 0.75 ml KN4.5 buffer, followed by inserting the column with the ABICAP® filter into the magnetic reader apparatus for measurement at room temperature (Fig. 1). The wash step and the measurements were conducted within 10 min.

2.7. Data evaluation

Data points in Figs. 3 and 4 were fitted by non-linear regression analysis (program Grafit version 3.04, Erithacus Software) using the equation for a single ligand binding site: $signal_{obs} = signal_{max}$[P RNA]/($K_d$ + [P RNA]), where $signal_{obs}$ = observed signal (mV − background), $signal_{max}$ = maximum signal [theoretical endpoint from the curve fit].

3. Results

Bacterial P RNAs are composed of two independent folding domains, the catalytic (C-) domain and the specificity (S-) domain [21,22] (Fig. 2). The S-domain confers specificity for precursor tRNAs (ptRNAs) by interacting with their T stem-loop region (for review, see [23]). The single bacterial P protein, dispensable *in vitro* but essential *in vivo* [24,25], binds to the C-domain of P RNA in the P2-J2/3-P3-J3/4-P4-J18/2 region (Fig. 2C) [26–29]. The protein increases substrate affinity through interaction with the 5′-leader [29,30], and confers tighter binding of key metal ions involved in substrate positioning and catalysis [31,32]. In contrast to bacterial P RNAs, their counterparts from archaea, eukarya and eukaryotic organelles have at best very low RNA-alone activity [8,33,34] which correlates with the presence of multiple protein subunits (usually 4 in Archaea and 9–10 in Eukarya). We recently fused the C-domain of the P RNA from the euryarchaeon *Methanothermobacter thermoautotrophicus* to the S-domain of *E. coli* P RNA. This was done in an attempt to reactivate RNA-alone activity of the archaeal C-domain by mutations towards the bacterial consensus, while simultaneously elevating the basal activity of the archaeal C-domain through combination with a fully proficient bacterial S-domain [13]. This type of chimeric P RNA was termed ME RNA, for *Methanothermobacter* C-domain and *E. coli* S-domain. A series of changes back to the bacterial P RNA consensus structure were then introduced into the C-domain of ME RNA, of which a few substantially improved the function of the ME chimera [13].

3.1. Measurements with chemagen beads type SAV 1 (NCO)

E. coli P RNA (EE RNA) as well as several ME RNA variants were analyzed for P RNA–protein interaction using streptavidin-coated magnetic beads from chemagen, type SAV 1 (NCO). The measured signals as a function of P RNA concentration resulted in reasonable binding curves for all RNAs except the least active ME RNA for which we expected low specific affinity for the *E. coli* P protein (see Discussion). Reasonable curve fits for a single ligand binding site gave K_d values between 0.8 nM for *E. coli* P RNA to approx. 330 nM for variant ME-mJ2/3 (Fig. 3). The value of 0.8 nM for *E. coli* P RNA nicely correlates with K_d values determined by independent methods under comparable conditions (0.4 nM; [10,11]). As expected, the ME variants had lower affinities than EE RNA for the *E. coli* P protein. After having performed the measurements presented in Fig. 3, our batch of chemagen type SAV 1 (NCO) beads was used up. Unfortunately, newly ordered batches from the same company failed to give reproducible P RNA concentration-dependent signals in the same experimental setup (data not shown), thus preventing us from conducting any further experiments with the type SAV 1 (NCO) beads. Microscopic

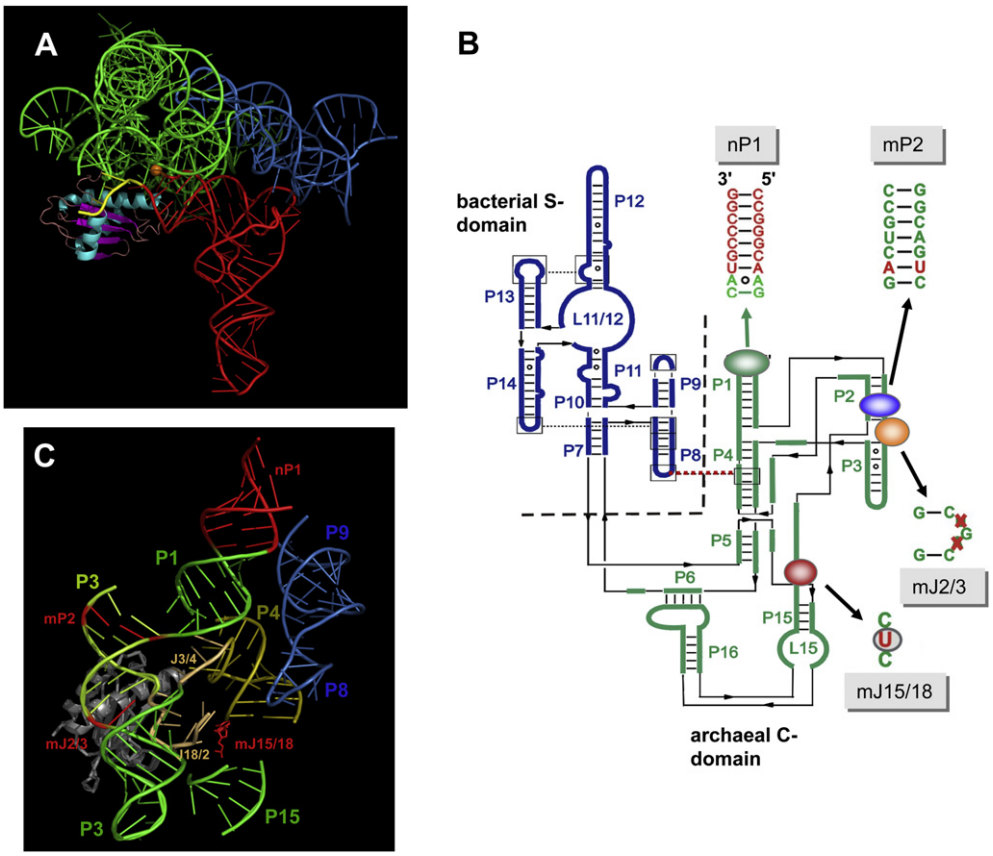

Fig. 2. (A) Model of RNase P-tRNA complexes based on the individual crystal structures of *B. stearothermophilus* P RNA (partial structure), *B. subtilis* P protein and yeast $tRNA^{Phe}$ [29]. The C-domain and the S-domain of P RNA are shown in green and blue, respectively. The tRNA is shown in red, with the 5′-terminal phosphate generated by RNase P cleavage depicted as orange sphere; the 3′-ACCA end of $tRNA^{Phe}$ is shown in yellow. The P protein is illustrated in the ribbon mode with α-helices in cyan, β-strands in magenta and loops in pink. (B) Secondary structure of the chimeric ME RNA illustrating the alterations mJ15/18, J2/3, mP2 and nP1 introduced into the archaeal C-domain. (C) Location of the alterations (in red) relative to the proposed binding site of the P protein (shown in grey ribbon mode), based on the model in panel A. (For interpretation of the references to colour in this figure legend, the reader is referred to the web version of this article.)

analyses (not shown) indicated that the magnetite (Fe_3O_4) of the new bead batches was partially oxidized to maghemite (Fe_2O_3) which leads to permanent magnetization of the beads.

3.2. Measurements with beads from other suppliers

We thus tested streptavidin-coated magnetic beads from other suppliers, including Dynal M-270, Seradyn MG-SA, and Estapor® BE-M0.8/26 magnetic beads (Fig. 4). For the Dynal M-270 beads, we additionally performed measurements with ABICAP® columns not coated with P protein as a control for non-specific RNA and streptavidin-coated magnetic bead adsorption to the ABICAP® filter surface. The obtained mV-Bkg values from this control experiment were additionally subtracted from the signals measured with P protein-coated columns at the corresponding P RNA concentration. The K_d value obtained from curve fitting (approx. 2.2 nM; Fig. 4A) was similar to the K_d determined for the Seradyn MG-SA 1.4 μm beads (2.3 nM; Fig. 4B), and in the same range (within 3-fold) as the K_d determined with chemagen type SAV 1 (NCO) beads (Fig. 3A). With the Estapor® beads, essentially no P RNA concentration-dependent signal relative to the blank value could be observed (Fig. 4C). Although the reasons for that remain unclear, the result provides another argument against non-specific adsorption of RNA and streptavidin-coated magnetic beads to the ABICAP® filter surface.

4. Discussion

4.1. Comparison of binding data with previous biochemical data

We recently measured complex formation between P RNA, P protein and ^{32}P-labeled ptRNA substrate using a spin column gel filtration (Sephadex G75) assay [13]. Under the applied low salt concentrations (200 mM NH_4OAc, 15 mM $Ca(OAc)_2$), ptRNA is unable to bind to P RNA alone; rather, complex formation of P RNA and P protein is a prerequisite for ptRNA binding. Thus, measured increases in substrate affinity also indirectly measured elevated P RNA–P protein affinities [13]. Table 1 compares the data for ptRNA substrate binding to the P RNA–P protein complex (=RNase P holoenzyme) with those for P RNA–P protein affinity measured directly by the magnetic sensor technique. We also included the observed rate constants for substrate cleavage in the holoenzyme reaction in the presence of the *E. coli* P protein. There is good correlation in the affinity/activity trends observed with all three assays, in the sense that *E. coli* (EE) RNA performed better (>) than ME-mJ15/18/2/3/P2/nP1 > ME-mJ15/18/2/3 ~ ME-mJ2/3/P2 > ME-mJ2/3. Such consistence of data consolidates our confidence that we measured biologically meaningful P RNA–P protein affinities with the magnetic sensor approach.

Since biochemical data pinpoint the P2-J2/3-P3-J3/4-P4-J18/2 region as the primary binding site for the bacterial P protein [26–29],

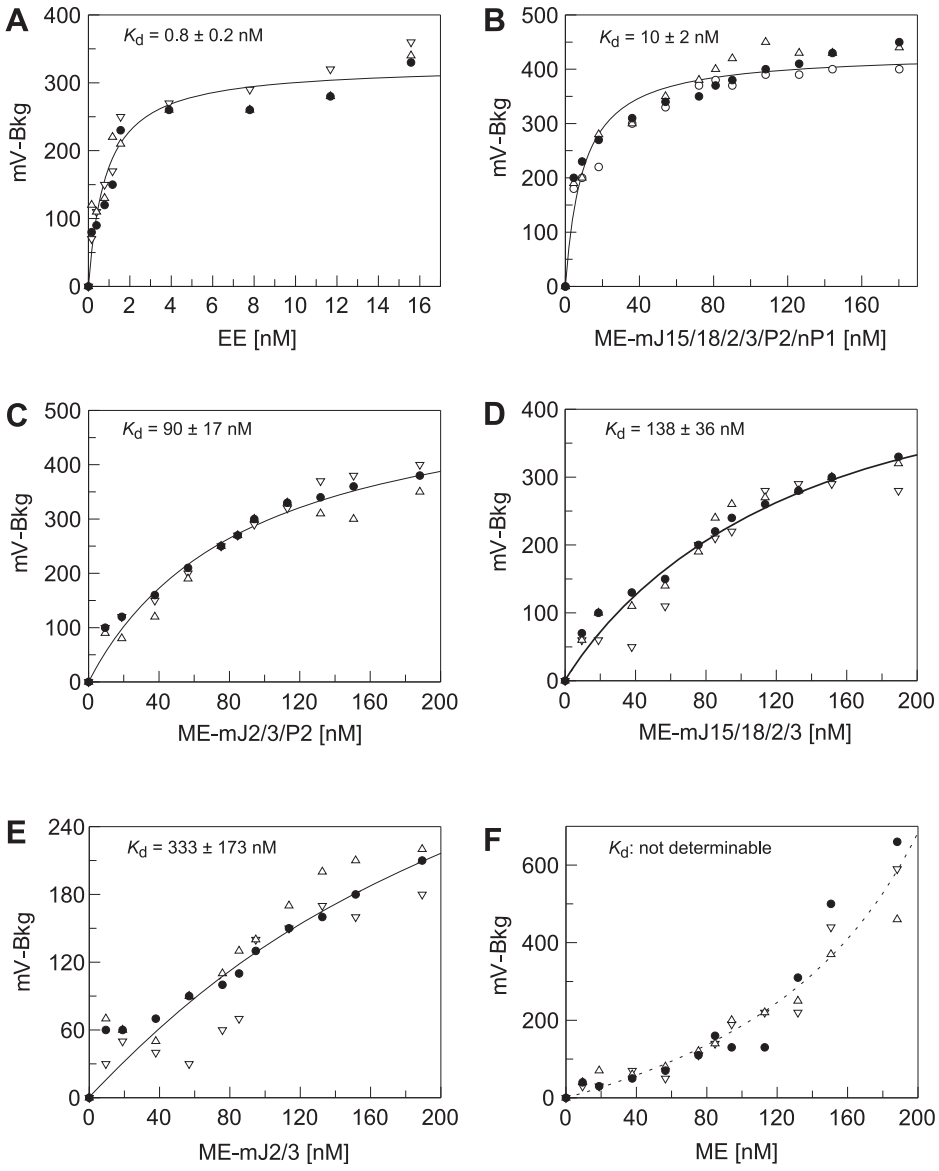

Fig. 3. (A–F): Magnetic sensor measurements as a function of concentration of different P RNA variants, using the chemagen SAV 1 (NCO) beads. Each graph includes data points from three independent experiments. Data were fitted to a single ligand binding curve using the program Grafit (see Materials and methods).

we introduced changes towards the bacterial consensus into this part of the archaeal C-domain (Fig. 2B and C, variants mJ2/3 and mJ2/3/P2). Variant ME-mJ2/3/P2 showed an increase in P protein affinity from non-determinable (variant ME) to a K_d of 90 ± 17 nM (Fig. 3C and F), providing further biochemical evidence that the P2/J2/3 region is a major determinant of the binding interface for the bacterial P protein. Surprisingly, almost equal P protein affinity was obtained for the variant combining the single C to U transition in J15/18 with the mJ2/3 mutation (K_d = 138 ± 36 nM; Fig. 3D). The molecular basis of this affinity enhancement is not clear at present. J15/18 is located at some distance to the protein binding interface according to current models (Fig. 2C), suggesting that the mJ15/18 transition mutation induces a conformational change of the catalytic domain, which improves P protein binding. Combining mutations mJ15/18, mJ2/3 and mP2 with a stabilizing extension of the terminal helix P1 resulted in variant ME-mJ15/18/2/3/P2/nP1 with a P protein affinity only approx. 10-fold lower than that of *E. coli* P RNA (EE RNA, Fig. 3A and B). An equal difference between the two RNAs was also seen for ptRNA substrate binding to the RNase P holoenzyme (Table 1).

4.2. Advantages and limitations of the magnetic sensor approach

We think we have convincingly demonstrated the applicability of the magnetic sensor technique to the study of specific RNA–protein interactions, with its strength in covering a rather broad affinity window (K_d values up to ~300 nM). However, we are aware that the magnetic biosensor requires validation from independent assays. This relates to the fact that the exact amount of binding-competent protein adsorbed to the sintered polyethylene filters cannot be assessed, which also precludes quantitation of the stoichiometry of RNA–protein complexes. Thus, results from independent approaches, such as gel shift assays, are needed as reference information. Also heterogeneity of RNA–protein complexes cannot be ruled out in magnetic biosensor assays.

As a practical drawback, we faced major problems with respect to the uniformity of bead batches from the same supplier, and beads from one provider gave no signal at all. We attribute this to the fact that streptavidin-coated magnetic beads are manufactured for biochemical separation purposes, but not for quantitative

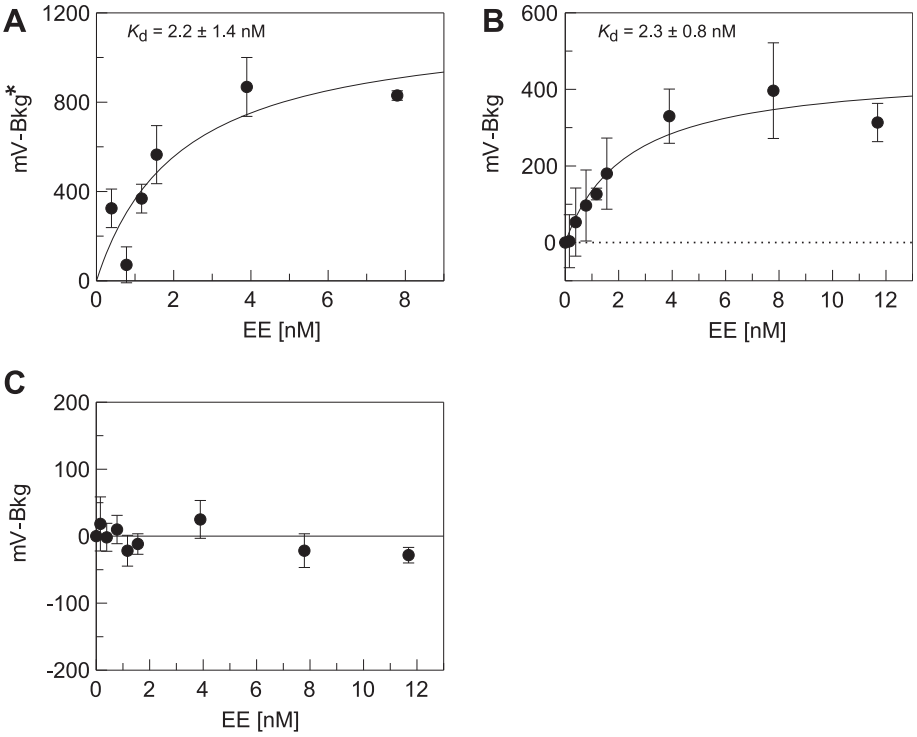

Fig. 4. Magnetic sensor measurements as a function of *E. coli* P RNA (EE) concentrations using streptavidin-coated magnetic beads from other suppliers. (A) Dynal M-270 beads; here, values obtained with ABICAP® columns not coated with P protein at the same P RNA concentration were subtracted in addition (indicated by "mV-Bkg*"). (B) Seradyn MG-SA and (C) Estapor® type BE-M0.8/26 magnetic beads. For further details, see legend to Fig. 3 and Materials and methods.

measurements requiring particles with defined and constant properties regarding particle diameter, surface chemistry, uniformity of streptavidin coating and particularly exclusion of non-magnetite ferrites. In fact, we see a major source of failure in possible maghemite (Fe_20_3) impurities of magnetite (Fe_30_4) beads, because maghemite spoils the superparamagnetic properties of the beads: maghemite is susceptible to permanent magnetization, resulting in magnetic attraction and aggregation of beads, such that the induced signals become independent of the specific RNA–protein interaction. Directed efforts towards manufacturing superparamagnetic beads for quantitative molecular interaction measurements would fill a gap in the repertoire of simple and robust biochemical analyses methods. For the time being, researchers applying magnetic sensor techniques are advised to either conduct their experimental series with a single functional batch of beads or to test different batches from the same supplier for reproducibility before the onset of their analyses.

Table 1
Comparison of K_d values for binding of the ptRNA^{Gly} substrate to RNase P holoenzymes and for P protein binding to P RNA.

RNase P RNA	Substrate K_d (nM)[a]	P RNA–P protein K_d	Holoenzyme k_{obs} [$min^{-1} \times 10^{-4}$][a]
EE	0.5 ± 0.1	0.8 ± 0.2	82 000 ± 2000
ME	n.d.	n.d.	2.0 ± 1.0
ME-mJ2/3	448 ± 30	333 ± 173	52 ± 6
ME-mJ2/3/P2	47 ± 11	90 ± 17	900 ± 200
ME-mJ15/18/2/3	48 ± 4	138 ± 36	320 ± 30
ME-mJ15/18/2/3/P2/nP1	5.0 ± 1.0	10 ± 2	3000 ± 500

Errors for K_d are standard errors of the curve fit; n.d., non-determinable because of affinities too low for K_d determination by the two assays (spin column gel filtration and magnetic sensor assay, respectively). For all variants ptRNA binding to P RNA in the absence of protein did not exceed background values (ptRNA alone).

[a] Data taken from [13]. Equilibrium dissociation constants (K_d) of complex formation between RNase P holoenzymes and ptRNA substrate (substrate K_d) were determined at 50 mM Tris–acetate, pH 7.1, 200 mM NH_4OAc, 0.05% Nonidet P-40, and 15 mM $Ca(OAc)_2$ using trace amounts (<1 nM) of 5′-^{32}P-labeled substrate. Holoenzyme activity assays were performed at 20 mM Hepes pH 7.4 at 37 °C, 2 mM spermidine, 0.05 mM spermine, 4 mM β-mercaptoethanol, 150 mM NH_4OAc, 4.5 mM $Mg(OAc)_2$, 100 nM ptRNA, 10 nM P RNA and 50 nM recombinant *E. coli* P protein with N-terminal His tag. Errors are standard deviations; all values are based on at least three independent experiments.

Acknowledgment

This work was supported by the Deutsche Forschungsgemeinschaft (HA 1672/14-1/3 and GRK 1384).

References

[1] A. Schön, Ribonuclease P: the diversity of a ubiquitous RNA processing enzyme. FEMS Microbiol. Rev. 23 (1999) 391–406.
[2] E. Hartmann, R.K. Hartmann, The enigma of ribonuclease P evolution. Trends Genet. 19 (2003) 561–569.
[3] S.C. Walker, D.R. Engelke, Ribonuclease P: the evolution of an ancient RNA enzyme. Crit. Rev. Biochem. Mol. Biol. 41 (2006) 77–102.
[4] D. Evans, S.M. Marquez, N.R. Pace, RNase P: interface of the RNA and protein worlds. Trends Biochem. Sci. 31 (2006) 333–341.
[5] C. Guerrier-Takada, K. Gardiner, T. Marsh, N. Pace, S. Altman, The RNA moiety of ribonuclease P is the catalytic subunit of the enzyme. Cell 35 (1983) 849–857.
[6] J.W. Brown, The ribonuclease P database. Nucleic Acids Res. 27 (1999) 314.
[7] R.K. Hartmann, M. Gössringer, B. Späth, S. Fischer, A. Marchfelder, The making of tRNAs and more – RNase P and tRNase Z. Prog. Mol. Biol. Transl. Sci. 85 (2009) 319–368.
[8] J.A. Pannucci, E.S. Haas, T.A. Hall, J.K. Harris, J.W. Brown, RNase P RNAs from some Archaea are catalytically active. Proc. Natl. Acad. Sci. U. S. A. 96 (1999) 7803–7808.
[9] H.Y. Tsai, D.K. Pulukkunat, W.K. Woznick, V. Gopalan, Functional reconstitution and characterization of *Pyrococcus furiosus* RNase P. Proc. Natl. Acad. Sci. U. S. A. 103 (2006) 16147–16152.
[10] A. Vioque, J. Arnez, S. Altman, Protein–RNA interactions in the RNase P holoenzyme from *Escherichia coli*. J. Mol. Biol. 202 (1988) 835–848.
[11] S.J. Talbot, S. Altman, Gel retardation analysis of the interaction between C5 protein and M1 RNA in the formation of the ribonuclease P holoenzyme from *Escherichia coli*. Biochemistry 33 (1994) 1399–1405.

[12] J.J. Day-Storms, S. Niranjanakumari, C.A. Fierke, Ionic interactions between PRNA and P protein in *Bacillus subtilis* RNase P characterized using a magnetocapture-based assay. RNA 10 (2004) 1595–1608.
[13] D. Li, D.K. Willkomm, R.K. Hartmann, Minor changes largely restore catalytic activity of archaeal RNase P RNA from *Methanothermobacter thermoautotrophicus*. Nucleic Acids Res. 37 (2009) 231–242.
[14] S. Busch, L.A. Kirsebom, H. Notbohm, R.K. Hartmann, Differential role of the intermolecular base-pairs G292-C(75) and G293-C(74) in the reaction catalyzed by *Escherichia coli* RNase P RNA. J. Mol. Biol. 299 (2000) 941–951.
[15] H.-J. Krause, N. Wolters, Y. Zhang, A. Offenhaüsser, P. Miethe, M.H.F. Meyer, M. Hartmann, M. Keusgen, Magnetic particle detection by frequency mixing for immunoassay applications. J. Magn. Magn. Mat. 311 (2007) 436–444.
[16] M.H. Meyer, M. Hartmann, H.J. Krause, G. Blankenstein, B. Mueller-Chorus, J. Oster, P. Miethe, M. Keusgen, CRP determination based on a novel magnetic biosensor. Biosens. Bioelectron. 22 (2007) 973–979.
[17] M.H. Meyer, M. Stehr, S. Bhuju, H.J. Krause, M. Hartmann, P. Miethe, M. Singh, M. Keusgen, Magnetic biosensor for the detection of *Yersinia pestis*. J. Microbiol. Methods 68 (2007) 218–224.
[18] D.K. Willkomm, R.K. Hartmann, 3'-Terminal attachment of fluorescent dyes and biotin. in: R.K. Hartmann, A. Bindereif, A. Schön, E. Westhof (Eds.), Handbook of RNA Biochemistry. WILEY-VCH, Weinheim, Germany, 2005, pp. 86–93.
[19] M.M. Bradford, A rapid and sensitive method for the quantitation of microgram quantities of protein utilizing the principle of protein–dye binding. Anal. Biochem. 72 (1976) 248–254.
[20] Inke Degener, 2004, Entwicklung von Methoden zur Immobilisierung von Polymersinterkörpern – Immunoassays für die pharmazeutische und lebensmittelchemische Qualitätskontrolle, PhD thesis, Bonn, Germany.
[21] A. Loria, T. Pan, Domain structure of the ribozyme from eubacterial ribonuclease P. RNA 2 (1996) 551–563.
[22] A. Loria, T. Pan, Recognition of the T stem-loop of a pre-tRNA substrate by the ribozyme from *Bacillus subtilis* ribonuclease P. Biochemistry 36 (1997) 6317–6325.
[23] L.A. Kirsebom, RNase P RNA mediated cleavage: substrate recognition and catalysis. Biochimie 89 (2007) 1183–1194.
[24] P. Schedl, P. Primakoff, J. Roberts, Processing of *E. coli* tRNA precursors. Brookhaven Symp. Biol. 26 (1974) 53–76.
[25] M. Gößringer, R. Kretschmer-Kazemi Far, R.K. Hartmann, Analysis of RNase P protein (*rnpA*) expression in *Bacillus subtilis* utilizing strains with suppressable *rnpA* expression. J. Bacteriol. 188 (2006) 6816–6823.
[26] R. Biswas, D.W. Ledman, R.O. Fox, S. Altman, V. Gopalan, Mapping RNA–protein interactions in ribonuclease P from *Escherichia coli* using disulfide-linked EDTA-Fe. J. Mol. Biol. 296 (2000) 19–31.
[27] H.Y. Tsai, B. Masquida, R. Biswas, E. Westhof, V. Gopalan, Molecular modeling of the three-dimensional structure of the bacterial RNase P holoenzyme. J. Mol. Biol. 325 (2003) 661–675.
[28] C. Rox, R. Feltens, T. Pfeiffer, R.K. Hartmann, Potential contact sites between the protein and RNA subunit in the *Bacillus subtilis* RNase P holoenzyme. J. Mol. Biol. 315 (2002) 551–560.
[29] A.H. Buck, A.V. Kazantsev, A.B. Dalby, N.R. Pace, Structural perspective on the activation of RNase P RNA by protein. Nat. Struct. Mol. Biol. 12 (2005) 958–964.
[30] J.C. Kurz, S. Niranjanakumari, C.A. Fierke, Protein component of *Bacillus subtilis* RNase P specifically enhances the affinity for precursor-tRNA^{Asp}. Biochemistry 37 (1998) 2393–2400.
[31] J.C. Kurz, C.A. Fierke, The affinity of magnesium binding sites in the *Bacillus subtilis* RNase P × pre-tRNA complex is enhanced by the protein subunit. Biochemistry 41 (2002) 9545–9558.
[32] L. Sun, M.E. Harris, Evidence that binding of C5 protein to P RNA enhances ribozyme catalysis by influencing active site metal ion affinity. RNA 13 (2007) 1505–1515.
[33] E. Kikovska, S.G. Svärd, L.A. Kirsebom, Eukaryotic RNase P RNA mediates cleavage in the absence of protein. Proc. Natl. Acad. Sci. U. S. A. 104 (2007) 2062–2067 Erratum in: Proc. Natl. Acad. Sci. USA 106 (2009) 8078.
[34] D. Li, D.K. Willkomm, A. Schön, R.K. Hartmann, RNase P of the *Cyanophora paradoxa* cyanelle: a plastid ribozyme. Biochimie 89 (2007) 1528–1538.